Paraelectric and ferroelectric phases of betaine phosphite: structural, thermodynamic, and dielectric properties

I. Fehst, M. Paasch, S. L. Hutton, M. Braune, R. Böhmer, Alois Loidl, M. Dörffel, Th. Narz, S. Haussühl, G. J. Mcintyre

Angaben zur Veröffentlichung / Publication details:

Fehst, I., M. Paasch, S. L. Hutton, M. Braune, R. Böhmer, Alois Loidl, M. Dörffel, Th. Narz, S. Haussühl, and G. J. Mcintyre. 1993. "Paraelectric and ferroelectric phases of betaine phosphite: structural, thermodynamic, and dielectric properties." *Ferroelectrics* 138 (1): 1–10. https://doi.org/10.1080/00150199308017710.

PARAELECTRIC AND FERROELECTRIC PHASES OF BETAINE PHOSPHITE: STRUCTURAL, THERMODYNAMIC, AND DIELECTRIC PROPERTIES

I. FEHST, M. PAASCH, S. L. HUTTON and M. BRAUNE
Institut für Physik, Johannes Gutenberg-Universität, 6500 Mainz, Germany

and

R. BÖHMER and A. LOIDL
Institut für Festkörperphysik, Technische Hochschule, 6100 Darmstadt, Germany

and

M. DÖRFFEL, TH. NARZ, and S. HAUSSÜHL
Institut für Kristallographie, Universität zu Köln, 5000 Köln, Germany

and

G. J. McINTYRE
Institut Laue-Langevin, 156X, 38042 Grenoble, France

The paraelectric and ferroelectric phases of betaine phosphite [BPI: $(CH_3)_3NCH_2COO \cdot H_3PO_3$] single crystals have been studied. The structure of BPI was determined at room temperature using x-ray and elastic neutron diffraction. Details of the ferroelectric transition and various low temperature properties were investigated using broad-band dielectric spectroscopy and calorimetric experiments. We compare the results obtained for single crystals of different origin which exhibit different ferroelectric phase transition temperatures.

I. INTRODUCTION

The betaine addition compounds belong to a class of complex crystals which show a fascinating variety of ordered low temperature states.[1,2] The occurrence of ferroelectricity[3] and ferroelasticity[4,5] has been reported for some of these solids, and also the formation of incommensurate superstructures.[6] An example of antiferroelectric ordering is found in betaine phosphate (BP).[7] Although synthesized first in 1914 this compound has been investigated in detail only in recent years.[7-14]

BP bears a number of similarities with representatives of the well-known KH_2PO_4

(KDP) family[15] in which the establishment of the ordered phases is triggered by the dynamics of the four hydrogen bonds linking the phosphate groups. In BP, on the other hand, two of the H-bridges emerging from the PO_4^{2-} tetrahedra serve to bond the amino acid betaine, and hence only two hydrogens connect to the adjacent phosphate groups.[13] It is interesting to study the dynamic behavior of these quasi-linear hydrogen-phosphate chains which may well be different from the dynamics of the three-dimensional network characterizing the KDP compounds.

Additional interest in the antiferroelectric BP stems from the fact that it is structurally very similar[8] to the ferroelectric betaine arsenate (BA).[16,17] Therefore it is not surprising that BP and BA form a complete series of solid solutions in which competing electrical dipole-dipole interactions lead to a frustrated low-temperature state.[18] Betaine phosphite (BPI), yet another ferroelectric member of this family of amino acid compounds[19] also forms mixed crystals with BP[20,21] in confirmation of suggestions by Albers *et al.*[19] Again a proton glass state was found to exist at intermediate concentrations.[20,21] These observations indicate the close structural affinity of BPI to the phosphate and arsenate compounds.

Like the other betaine compounds BP and BA, betaine phosphite exhibits a high-temperature paraelastic phase. Below a second order elastic phase transition at $T_{c1} = 365$ K[19] the betaine molecules arrange in an antiferrodistortive pattern. The paraelectric-to-ferroelectric transformation shows up at $T_{c2} = 216$ K or other temperatures depending on the growth conditions.[19]

Apart from the results of the initial characterization, reported along with the recent discovery of BPI,[19] not much is known about this ferroelectric. Therefore we have used x-ray[22] and elastic neutron diffractometry, adiabatic calorimetry, and broadband dielectric spectroscopy in order to elucidate further the static and dynamic properties of BPI single crystals.

II. RESULTS AND DISCUSSION

A. Sample Preparation

BPI single crystals were grown by controlled evaporation from aqueous solutions of the α amino acid betaine (B) and phosphoric acid H_3PO_3 (PI) at a growth temperature of 315 K. The molar ratio B:PI in the solution was 1:1.

Dielectric measurements were performed on samples originating from two different laboratories. Crystal 1 was grown by J. Albers in Saarbrücken while crystal 2 was prepared by one of the authors in Köln under similar conditions, in particular with the same molar ratio of B:PI in the solution. The ferroelectric phase transition temperatures T_{c2} of the two crystals differ by roughly 20 K; sample 1 shows the transition at $T_{c2} = 220$ K while in the second sample it is seen at 196 K.

B. Single Crystal Diffraction

The structure of betaine phosphite was determined using x-ray diffraction[22] and elastic neutron scattering experiments. The latter were performed on the four-circle spectrometer D10 at the Institut Laue Langevin in Grenoble using an optically

clear single crystal (sample 1). This crystal was characterized by dielectric and calorimetric measurements, as described below, and was found to exhibit an electric ordering transition at T_{c2} = 220 K in accord with previous reports.[19]

At room temperature 2084 reflections were recorded in the ω-2Θ scan mode at a neutron wavelength of 1.2600(5) Å. The raw data were corrected for absorption and extinction. The monoclinic unit cell in the paraelectric phase (space group $P2_1/c$) revealed the lattice parameters a = 11.267(5) Å, b = 7.607(5) Å, c = 12.467(8) Å, and β = 116.27(4)° at room temperature. Structural refinement was performed using the UPALS computer program[23] and yielded the atomic positions given in Table I. The refinement converged at a conventional R factor of 0.083. The atomic positions together with the experimentally determined temperature factors were used to generate the ORTEP plot of the asymmetric unit of BPI shown in the upper frame of Figure 1.

A comparison of our results from neutron scattering (sample 1) with those of the previous x-ray investigation (sample 2) shows that the lattice constants b and c from both experiments practically agree within the error bars. Small but significant deviations show up for the parameters a and β. The positions of the non-hydrogen atoms from both studies are in reasonable agreement with each other. Significant deviations seem to occur for the hydrogen atoms. In view of the fact that neither with x-ray nor with neutron diffractometry the positions of the hydrogen atoms

TABLE I

Atomic coordinates of BPI at 290 K (neutron data). The standard deviations are given in brackets. Note that the site occupation of H13 and H15 is 0.5.

Atom	x	y	z
O1	0.0404(1)	0.2301(3)	0.4169(1)
O2	1.0085(1)	0.2427(4)	0.2273(1)
C5	0.9688(1)	0.2430(2)	0.3105(1)
C4	0.8198(1)	0.2657(2)	0.2555(1)
N	0.75866(9)	0.2639(1)	0.34009(8)
C1	0.6132(1)	0.2910(3)	0.2660(2)
C2	0.7788(2)	0.0911(2)	0.4032(2)
C3	0.8096(2)	0.4104(3)	0.4288(2)
H1	0.5977(4)	0.4161(7)	0.2214(4)
H2	0.5762(3)	0.1885(8)	0.1997(4)
H3	0.5650(3)	0.2860(8)	0.3243(4)
H4	0.7242(5)	0.0923(6)	0.4542(5)
H5	0.7455(6)	-0.0118(6)	0.3373(6)
H6	0.8824(5)	0.0751(6)	0.4627(5)
H7	0.7514(5)	0.4130(6)	0.4786(4)
H8	0.9116(5)	0.3860(6)	0.4896(4)
H9	0.7977(5)	0.5316(6)	0.3826(5)
H10	0.7943(3)	0.3924(5)	0.2090(3)
H11	0.7736(3)	0.1619(5)	0.1903(3)
P	0.3601(1)	0.2539(2)	0.4186(1)
O3	0.2513(1)	0.1980(2)	0.3013(2)
O4	0.4877(2)	0.1486(3)	0.4555(2)
H14	0.3199(3)	0.2268(6)	0.5089(3)
O6	0.3908(2)	0.4485(2)	0.4209(2)
H12	0.1120(3)	0.2284(5)	0.2631(3)
H13	0.503(1)	0.0347(8)	0.497(1)
H15	0.517(2)	0.500(5)	0.518(1)

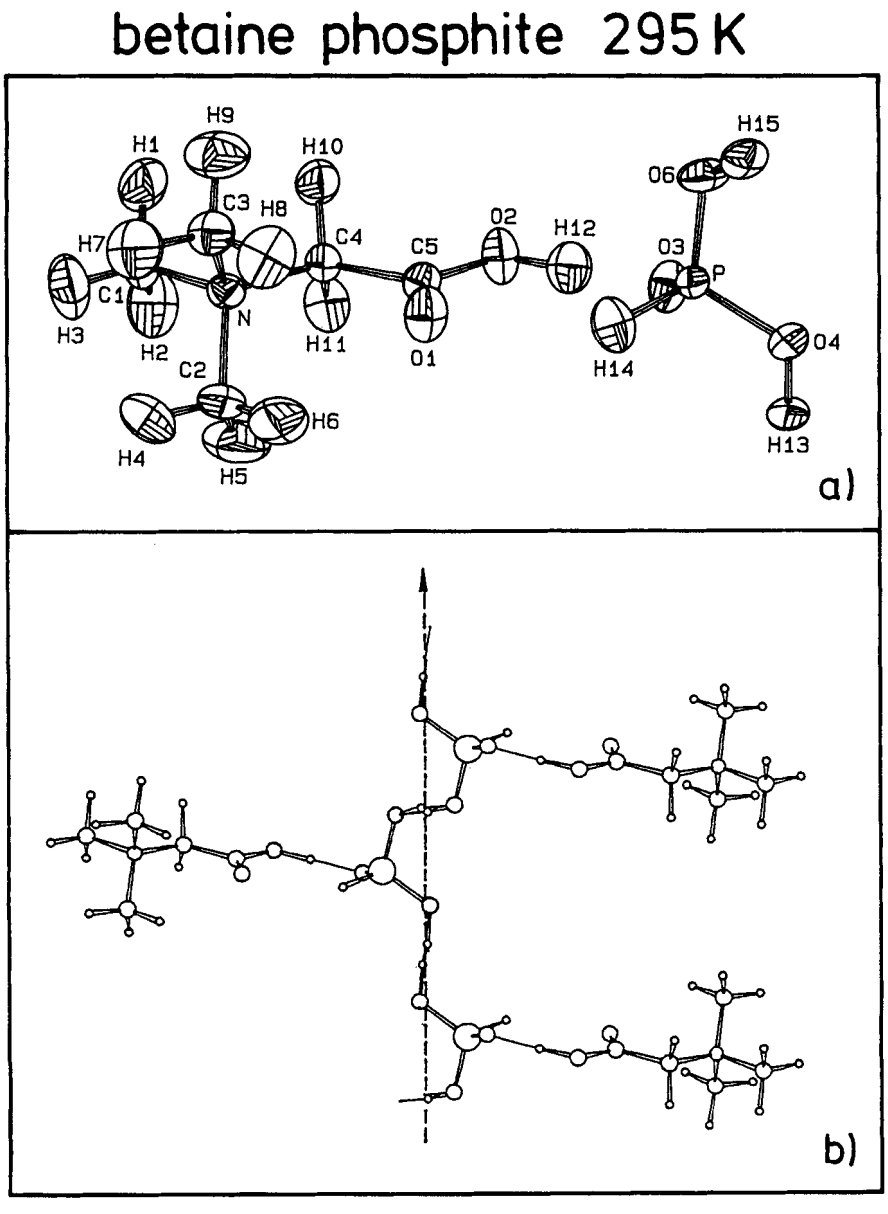

FIGURE 1 Upper frame: ORTEP plot of BPI according to the atomic positions given in Table I. Lower frame: Schematic drawing of the netting of the BPI units. The dashed line represents the monoclinic [010] axis.

can be determined with high precision, we can however not decide at present whether these deviations reflect intrinsic differences of the samples or merely are due to the underestimation of the error bars which are based on the counting statistics only.

In view of the relatively small differences of some lattice parameters of samples 1 and 2 the relatively large difference in their transition temperatures T_{c2} may be

somewhat surprising. We note however that in some ferroelectrically ordering compounds also minute amounts of impurities, which can easily escape the detection by diffraction techniques, are able to change the transition temperature substantially. As an example we mention that the addition of less than 1% of Fe ions lowers the upper ferroelectric transition temperature of $BaTiO_3$ by about 20 K.[24]

The ORTEP plot shown in Figure 1 documents the structural affinity of BPI to the well studied compound BP.[8] In contrast to BP, in BPI the hydrogen atom H12 forms hydrogen bonds from the oxygen O2 in the organic part to O3 located in the inorganic component. The oxygen atom O5 which in BP is attached to the P atom, in BPI is replaced by H14. Thus only one hydrogen bridge connects the amino acid to the inorganic part of the molecule.

Figure 1b shows how the molecular units depicted in Figure 1a are interconnected via the hydrogens H13 and H15. It is interesting to note that the H13—O4 bond is almost parallel to the ferroelectric axis (*b*-direction), while the H15—O6 bond is almost perpendicular to it.

C. *Dielectric Experiments*

The complex dielectric permittivity $\varepsilon = \varepsilon_1 - i\varepsilon_2$ was measured along the monoclinic *b* direction of gold-plated crystal slabs cut to dimensions of roughly $9 \times 7 \times 2.5$ mm^3. Using several impedance analyzers (HP4191, HP4192, and HP4274) the frequency range $10\ Hz \leq f \leq 1\ GHz$ was covered. The experiments were performed using a conventional He-flow cryostat and closed-cycle refrigerator systems. Sample temperatures were measured using calibrated silicon diodes.

Figure 2 shows the results obtained for sample 2 (with $T_{c2} = 196$ K). The cooling of the paraelectric phase is accompanied by a strong increase of the dielectric constant ε_1 (Figure 2a). The cusp in ε_1 at T_{c2} is characteristic for a second order phase transition which is often found to occur in order-disorder ferroelectrics.[15] Considerable dielectric loss is observed near the ferroelectric phase transition (Figure 2b). The dielectric loss ε_2 is almost frequency independent ($\varepsilon_2 \sim f^{s-1}$ with $s \rightarrow 1$ close to unity). Small Debye loss peaks are superimposed on this background. The relaxation times of the Debye processes were found to follow Arrhenius laws with inverse attempt frequencies of the order of 1 ps and energy barriers of the order of 2500 K. The relaxation strengths of the Debye processes shows a maximum at T_{c2}. This suggests that their dynamics, possibly being due to the relaxation of the organic sidegroups,[25] are coupled to the ferroelectric ordering.

For sample 2 the peak value of the permittivity as measured at 196 K is about 6000. This value is considerably smaller than the maximum dielectric constant reported by Albers *et al.*[19] and that found for sample 1 in the present work. In accord with our discussion of the structural investigations we interpret this decrease in $\varepsilon_{1,max}$ as an impurity effect which can be quite pronounced in order-disorder ferroelectrics.

In Figure 3 we have plotted the temperature dependence of the inverse dielectric constant ε_1^{-1} of both, sample 1 and sample 2. This plot clearly shows that the electric ordering temperatures measured for the two samples differ by about 20 K. Also the shape of the $\varepsilon_1^{-1}(T)$ curves though slightly different for the two crystals,

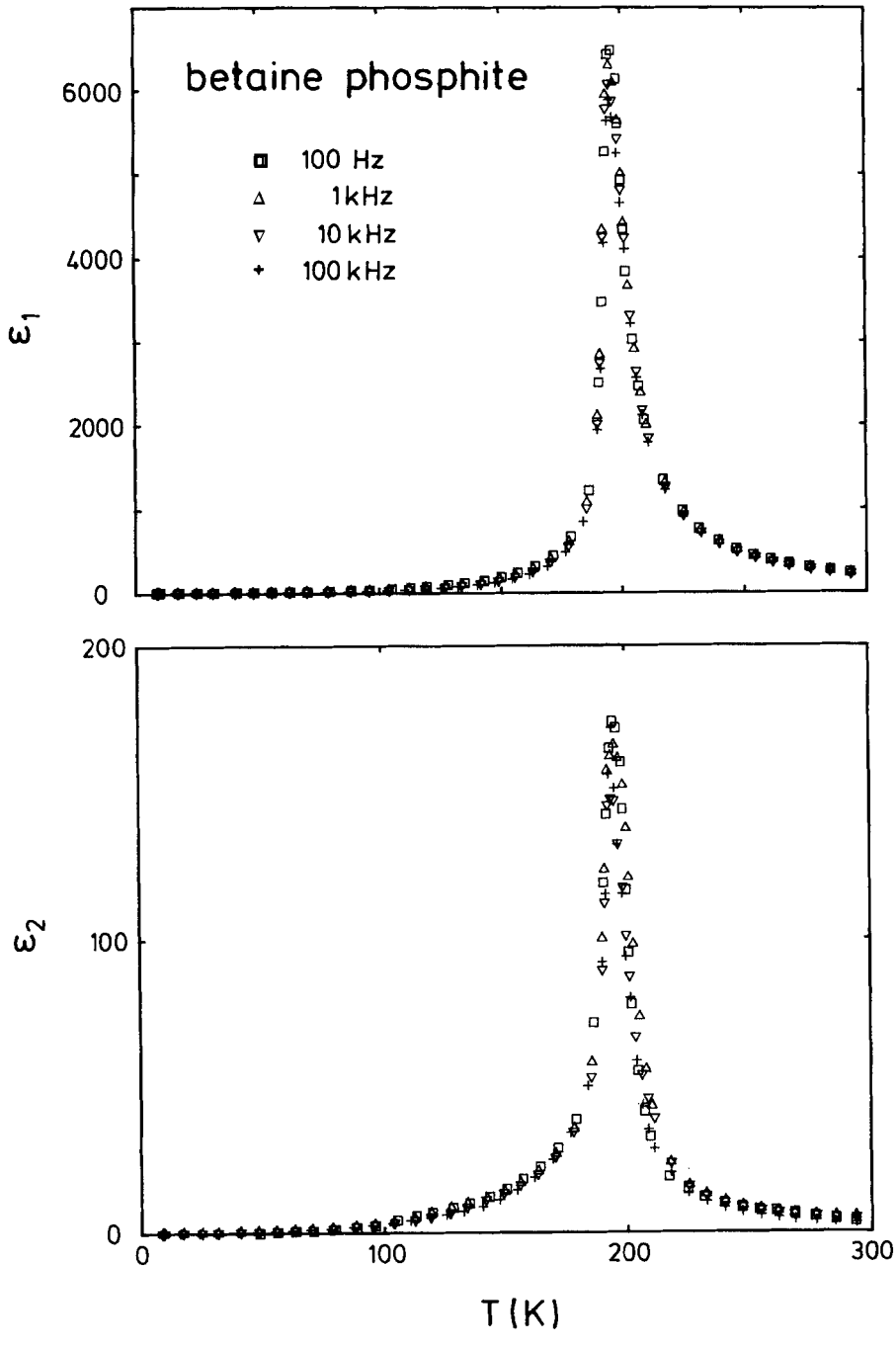

FIGURE 2 The temperature dependence of the complex dielectric constant of BPI (sample 2) measured at frequencies (10^2 Hz $\leq \nu \leq 10^5$ Hz). The upper and the lower frames show the real and imaginary part, respectively.

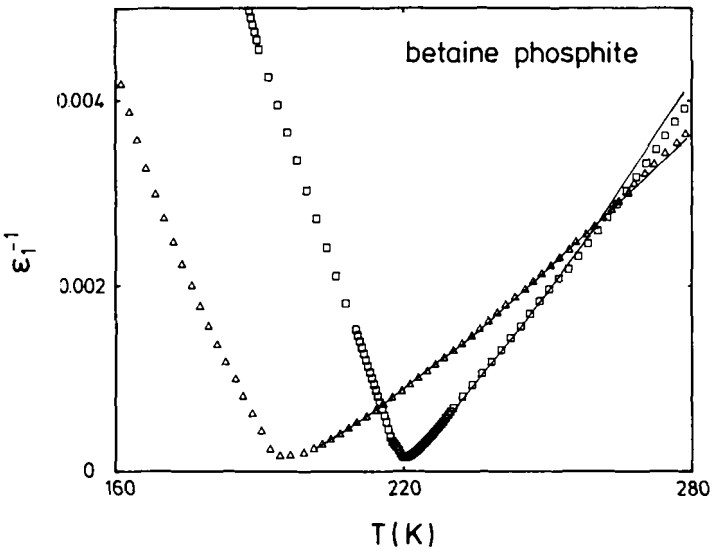

FIGURE 3 Inverse dielectric permittivity of BPI single crystals as measured along the monoclinic axes of BPI single crystals (squares: sample 1; triangles: sample 2). Solid lines are calculated using the anisotropic Ising model (Equation 1) with the parameters given in the text.

at first glance indicates Curie-Weiss (i.e. linear) behavior in both cases. A closer inspection however reveals deviations from the linear T-dependence of ε_1^{-1} even in the vicinity of T_{c2}.

Such a behavior might indicate increasing correlations[26] among the motions of the hydrogens connecting the phosphate groups as the temperature is lowered. However, the strongly anisotropic Ising model, previously applied to the antiferroelectric BP and other betaine compounds,[13] also gives rise to deviations from Curie-Weiss behavior. In the quasi-one-dimensional Ising model the coupling along the chain ($J_\parallel$) is much stronger than that perpendicular to it ($J_\perp$). Treating the intrachain coupling $J_\parallel$ rigorously and applying the mean field approximation for the interchain coupling $J_\perp$ yields, for temperatures above the electric transition[27]

$$\varepsilon_1 - \varepsilon_\infty = C/[T \exp(-2J_\parallel/T) - J_\perp]. \quad (1)$$

Here the coupling constants as well as the Curie constant C are given in units of temperature. For the temperature range shown in Figure 3 the high-frequency dielectric constant ε_∞ is certainly much smaller than ε_1. Therefore trial fits with $\varepsilon_\infty \leq 100$ produced only minor variations in the fitted values of the coupling constants. Since an unambiguous determination of ε_∞ (which may be temperature dependent[28]) is difficult on the basis of the present data, in the following we have set ε_∞ to zero.

Equation (1) provides a good fit to our experimental results, see Figure 3. The solid lines in this figure were determined using least square fits and yielded for sample 1: $J_\parallel = 260$ K, $J_\perp = 20.5$ K and for sample 2: $J_\parallel = 215$ K, $J_\perp = 21.5$ K. Thus the transition temperatures T_{c2} of both samples are related to the strength of their intra-chain interactions by $T_{c2} = (0.88 \pm 0.04)\, J_\parallel$. The anisotropy in the coupling constants of BPI $J_\parallel/|J_\perp| = 11.3 \pm 1.2$ within experimental errors is identical to that of BP.[13] Of course in the ferroelectric compound BPI we find $J_\perp > 0$ while $J_\perp$ carries the opposite sign for the antiferroelectric BP.[13]

D. *Adiabatic Calorimetry*

The heat-capacity experiments were carried out in a standard quasiadiabatic calorimeter[29] by applying Joule heat to the single crystalline specimen (sample 1) having a mass of approximately 1.4 g. The temperature versus time profiles were measured with germanium (3 K $\leq T \leq$ 50 K) and with platinum (20 K $\leq T \leq$ 300 K) resistance thermometers.

The heat capacity c_p for BPI is shown in Figure 4 for temperatures 3 K $< T <$ 250 K. The ferroelectric transition at 220 K shows up as a very weak anomaly only: at T_{c2} the heat capacity as a function of temperature exhibits a change of slope (inset to Figure 4). The data presented in Figure 4 provide experimental evidence that the entropy changes ΔS at the FE phase transition are rather small, or are smeared out over a large temperature range. The latter possibility seems unlikely in view of the sharpness of the transition as evidenced by the dielectric experiments. In BP the heat capacity shows two anomalies close to the electric ordering temperature (at 89 K and 81 K).[12,30] In BPI, neither in the c_p-data nor in the dielectric measurements, indications for a phase transition below T_{c2} could be detected.

Finally, Figure 5 shows the low-temperature heat capacity in more detail. c_p roughly follows a T^3-dependence which is expected for insulating crystals at low temperatures (Figure 5, upper frame). The solid lines in Figure 5 are calculated with the Debye model for the specific heat[29]

$$c_p(T) = 3fR(T/\Theta_D)^3 \int_0^{\Theta_D/T} dx\, x^4 e^x (e^x - 1)^{-2} \qquad (2)$$

using a Debye temperature $\Theta_D = 154$ K. In Equation (2) R denotes the gas constant and $f = 13.5 \pm 0.5$ the effective number of thermally excited degrees of freedom.

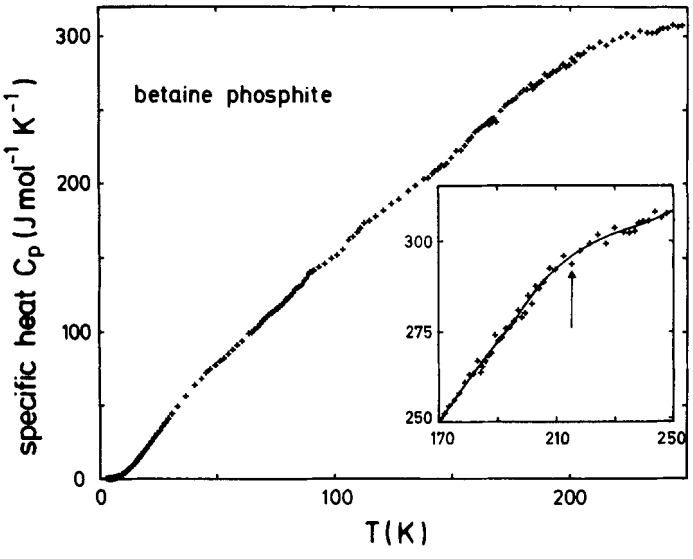

FIGURE 4 Temperature dependent specific heat of sample 1. The inset provides an enlarged view of the data obtained in the vicinity of the ferroelectric transition. T_{c2} as determined in dielectric experiments is marked by the arrow.

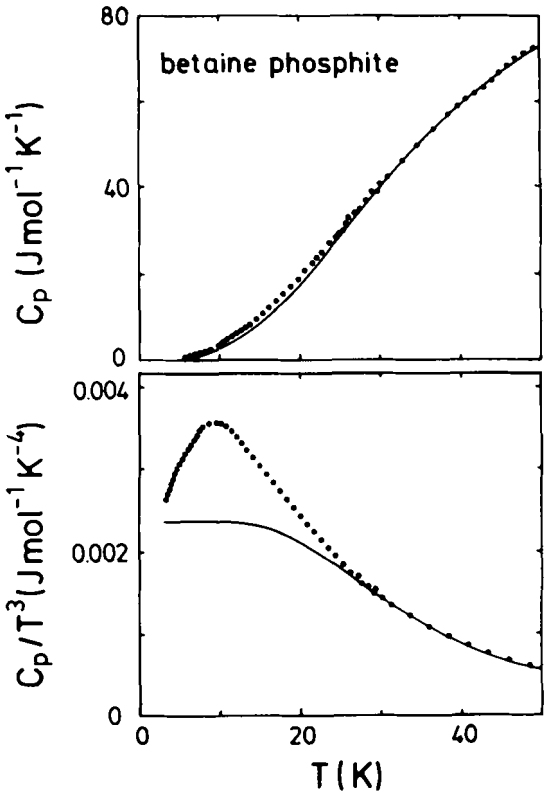

FIGURE 5 Low-temperature specific heat of BPI (sample 1) plotted as c_p (upper frame) and c_p/T^3 (lower frame) versus T. The experimental results are represented by the dots. The solid line is calculated using the Debye model for the specific heat (Equation (2)) with a Debye temperature Θ_D of 154 K.

The experimental results significantly deviate from the model calculations for temperatures near 15 K. To emphasize these deviations, in the lower frame of Figure 5 our c_p-data and the calculated Debye heat capacity are shown as c_p/T^3 versus T. Well defined excess contributions appearing in this representation usually indicate glass-like behavior[31,32] but have also been detected in ordered ferroelectrics.[32,33] The origin of the excess contributions in a number of these compounds thus far has remained unclear. For the case of betaine phosphite we note that the excess heat capacity may be due to low lying optical modes, yielding a high density of phonon states at low excitation energies.[34]

III. SUMMARY

We have investigated betaine phosphite single crystals from various sources. The structure of these crystals was studied using x-ray and elastic neutron diffraction techniques. It was shown that the molecular units of BPI possess a close structural affinity to those from which betaine phosphate is constituted. The results from the crystallographic investigations of the two crystals revealed small but significant differences of some lattice parameters which may be related to the difference of

the ferroelectric transition temperatures (of about 20 K) as seen in the dielectric experiments. The permittivities measured in the paraelectric phases of the different samples could be described in the framework of the anisotropic Ising model with nevertheless almost identical parameters. Using a least squares procedure we find an intrachain coupling strength of 1.14 T_c and an interchain coupling which is about 11 times smaller.

The ferroelectric anomaly was also detected using adiabatic calorimetry. However the small transition entropy associated with the transition rendered a quantitative evaluation of the data taken around T_c impossible. An analysis of the low temperature specific heat ($T < 50$ K) was performed in terms of the Debye model yielding a Debye temperature of 154 K. Excess heat capacity contributions which have previously been reported to show up in many ferroelectrics have also been detected for BPI.

REFERENCES

1. J. Albers, *Ferroelectrics*, **78,** 3 (1988).
2. D. Schaack, *Ferroelectrics*, **104,** 147 (1990).
3. H. E. Müser and U. Schell, *Ferroelectrics*, **55** 279 (1984).
4. S. Haussühl, *Solid State Commun.*, **50,** 63 (1984).
5. S. Haussühl, *Solid State Commun.*, **68,** 963 (1988).
6. H. J. Rother, J. Albers and A. Klöpperpieper, *Ferroelectrics*, **54,** 107 (1984).
7. J. Albers, A. Klöpperpieper, H. J. Rother and K. H. Ehses, *Phys. Stat. Sol. (a)*, **74,** 553 (1982).
8. W. Schildkamp and J. Spilker, *Z. Kristallogr.*, **168,** 159 (1984).
9. H. Ohki, N. Nakamura and H. Chihara, *Ferroelectrics Lett.*, **8,** 19 (1987).
10. M. Maeda, *J. Phys. Soc. Jpn.*, **57,** 3059 (1988).
11. K. Hara, H. Umeda, Y. Ishibashi, and I. Suzuki, *J. Phys. Soc. Jpn.*, **58,** 4215 (1989).
12. M. Maeda, T. Atake, Y. Saito and H. Terauchi, *J. Phys. Soc. Jpn. Lett.*, **58,** 1135 (1989).
13. G. Fischer, H. J. Brückner, A. Klöpperpieper, H.-G. Unruh and A. Levstik, *Z. Phys. B*, **79,** 301 (1990).
14. G. Völkel, A. Pöppl, H. Metz and A. Klöpperpieper, *Ferroelectrics*, **125,** 11 (1992).
15. e. g. F. Jona and G. Shirane, *Ferroelectric Crystals* (Pergamon, Oxford, 1962), Chapt. 3.
16. U. Schell and H. E. Müser, *Z. Phys. B*, **66,** 237 (1987).
17. M. Maeda, *J. Phys. Soc. Jpn.*, **57,** 2162 (1988).
18. M. Maeda, *Ferroelectrics*, **96,** 269 (1989).
19. J. Albers, A. Klöpperpieper, H. J. Rother and S. Haussühl, *Ferroelectrics*, **81,** 27 (1988).
20. M. L. Santos, J. C. Azevedo, A. Almeida, M. R. Chaves, A. R. Pires, H. E. Müser and A. Klöpperpieper, *Ferroelectrics*, **108,** 363 (1990).
21. S. L. Hutton, I. Fehst, R. Böhmer, M. Braune, B. Mertz, P. Lunkenheimer and A. Loidl, *Phys. Rev. Lett.*, **66,** 1990 (1991).
22. M. Dörffel, Th. Narz, and S. Haussühl, *Z. Kristallogr.*, **186,** 71 (1989).
23. J.-O. Lundgren, *Crystallographic Computer Programs, Report UUIC-B13-04-05*, Institute of Chemistry, University of Uppsala, Sweden, 1982.
24. M. Maglione, R. Böhmer, A. Loidl and U. T. Höchli, *Phys. Rev. B*, **40,** 11441 (1989).
25. S. L. Hutton, I. Fehst and A. Loidl, *Ber. Bunsenges. Phys. Chem.*, **95,** 1037 (1991).
26. R. Böhmer, P. Lunkenheimer, J. K. Vij and I. Svare, *J. Phys.*, **2,** 5433 (1990).
27. A. Levstik, B. Zeks, I. Levstik, H. G. Unruh, G. Luther and H. Roemer, *Phys. Rev. B*, **27,** 5706 (1983).
28. O. Freitag, H. J. Brückner and H.-G. Unruh, *Z. Phys. B*, **61,** 75 (1985).
29. B. Mertz, Dissertation, Mainz (1990).
30. M. Braune, Diplomarbeit, Mainz (1990).
31. B. Mertz, R. Böhmer, B. Eisele and A. Loidl, *Z. Phys. B*, **79,** 431 (1990).
32. W. N. Lawless, D. Rytz and U. T. Höchli, *J. Phys. C*, **17,** 2609 (1984).
33. G. Burns, *Solid State Commun.*, **35,** 811 (1980); E. Gmelin and G. Burns, *Phys. Rev. B*, **38,** 442 (1988).
34. Assuming an Einstein model for the specific heat, the energy of these excitations in BPI is estimated to be centered around 3–4 meV. Low lying optical modes have been found in inelastic neutron scattering experiments on other betaine compounds, cf. R. Currat, J. F. Legrand, S. Kamba, J. Petzelt, V. Dvorak and J. Albers, *Solid State Commun.*, **75,** 545 (1990).